Carbohydrate Polymers 85 (2011) 803–808

Contents lists available at ScienceDirect

Carbohydrate Polymers

journal homepage: www.elsevier.com/locate/carbpol

Preparation, characterization and *in vitro* release of chitosan nanoparticles loaded with gentamicin and salicylic acid

Jingou Ji[a,*], Shilei Hao[a], Danjun Wu[a], Rui Huang[b], Yi Xu[a]

[a] *Faculty of Pharmacy, College of Chemistry and Chemical Engineering, University of Chongqing, Chongqing 400030, China*
[b] *College of Bioengineering, University of Chongqing, Chongqing 400030, China*

ARTICLE INFO

Article history:
Received 15 May 2010
Received in revised form 24 February 2011
Accepted 31 March 2011
Available online 8 April 2011

Keywords:
Chitosan nanoparticles
Gentamicin
Ototoxicity
Salicylic acid
In vitro release

ABSTRACT

Salicylic acid (SA) and gentamicin (GM) loaded nanoparticles of chitosan (CS) cross-linked with tripolyphosphate (TPP) were prepared and used to inhibit the ototoxicity of GM. The prepared nanoparticles were characterized by FT-IR spectroscopy to confirm the cross-linking reaction between CS and cross-linking agent. X-ray diffraction (XRD) was performed to reveal the crystalline nature of the drug after encapsulation. Up to 24.67 ± 2.06% of SA and 26.64 ± 3.92% of GM were loaded into the nanoparticles and the average size of nanoparticles ranged from 148 ± 8.6 to 345.0 ± 12.9 nm. The nanoparticles formed were spherical in shape with high zeta potentials (higher than +30 mV). *In vitro* release studies in phosphate buffer saline (pH 7.4) showed an initial burst effect and followed by a slow drug release. The drug release followed Weibull equation and a non-Fickian transport. The amounts of SA and GM released from the nanoparticles met the dosage ratio requirement for inhibiting ototoxicity of GM by SA.

1. Introduction

Gemtamycin (GM) is an aminoglycoside antibiotic used for treating many types of bacterial infections, particularly those caused by Gram-negative bacteria. However, the side effects of GM, i.e. ototoxicity and nephrotoxicity, restrict its clinical application (Song, Sha, & Schacht, 1998). A number of researches have suggested that the free radicals were involved in the ototoxicity of GM (Hirose, Hockenbery, & Rubel, 1997; Polat et al., 2006; Ryals, Westbrook, & Schacht, 1997; Talaska, Schacht, & Nathan, 2006). Therefore, the free radical scavengers, such as glutathione, salicylic acid (SA), aspirin (acetyl salicylic acid), 2,3-dihydroxybenzoic acid, aminoguanidine and edaravone have been used to inhibit the ototoxicity of GM successfully (Lautermann, McLaren, & Schacht, 1995; Maekawa et al., 2009; McFadden, Ding, Salvemini, & Salvi, 2003; Severinsen, Kirkegaard, & Nyengaard, 2006). Aspirin has been used to antagonize GM ototoxicity in clinical trials (Chen et al., 2007).

In practice, GM is injected once daily while SA needs to be injected twice a day (Sha & Schacht, 2000). The multiple injections bring inconvenience for the patients. In addition, once the free radicals generate, they will immediately react with the vicinal macromolecules due to their highly activity. In order to effectively inhibit the ototoxicity of the free radicals of GM, scavengers need to be available to react with the free radicals as soon as they are produced. Separating injections may result in poor coordination of GM and SA *in vivo*, and consequently reduce the antagonism of SA.

A suitable delivery system such as the site-specific and controlled release delivery can improve the bioavailability of the drug and minimize their side effects (Govender et al., 2000). Research showed that nanoparticles were able to protect the drugs from degradation and controlled the release of the encapsulated or adsorbed drugs (Atyabi, Moghaddam, Dinarvand, ZohuriaanMehr, & Ponchel, 2008). The nanoencapsulation of medicinal drugs (nanomedicines) also has many advantages in the enhancement of absorption into a selected tissue and improvement of intracellular penetration, bioavailability and retention time, and therefore, both the cost of the drug use and the risk of the toxicity for patient could be reduced (Kumari, Yadav, & Yadav, 2010).

Polymeric materials such as chitosan (CS), poly-d, l-lactide-co-glycolide (PLGA) and polylactic acid (PLA) are used for synthesis of nanoparticles. CS is a naturally occurring and abundantly available polysaccharide. It is the *N*-deacetylation product of chitin (Cooney, Petermann, Lau, & Minteer, 2009; Peesan, Supaphol, & Rujiravanit, 2005). The relative molecular weight of CS ranges from hundreds of thousands to millions (Fu, Huang, Zhai, Li, & Liu, 2007). CS and its derivatives have been widely used in pharmaceutical and medical areas, due to its favorable biological properties such as good biocompatibility, biodegradability, antibacterial activity (No, Kim, Lee, Park, & Prinyawiwatkul, 2006), wound healing acceleration ability, fungistatic, anticancerogen, anticholesteremic and low toxicity (Fan, Hu, & Shen, 2009). LD_{50} of CS for laboratory mice is 16 g/kg body weight, which is close to that of sugar or salt (Agnihotri,

* Corresponding author. Tel.: +86 23 62235596.
E-mail address: jingou_ji@yahoo.com.cn (J. Ji).

0144-8617/$ – see front matter © 2011 Elsevier Ltd. All rights reserved.
doi:10.1016/j.carbpol.2011.03.051

Mallikarjuna, & Aminabhavi, 2004). CS derivatives are also found to possess good antioxidant activity (Lin & Chou, 2004). Therefore, CS nanoparticles are suitable to be used for the drug and gene delivery (Gan, Wang, Cochrane, & McCarron, 2005; Wan, Sun, Gao, & Li, 2009; Wang, Chi, & Tang, 2008). In addition, CS has special properties such as protonization under acidic condition due to its amino groups and can be cross-linked with anions such as tripolyphosphate (TPP) to form nanoparticles. The preparation of CS nanoparticles via the cross-linking method was found to be simple and mild.

In present study, the compound CS nanoparticles were synthesized by an ionic cross-linking method. GM and SA were loaded into the nanoparticles. The compound nanoparticles could release GM and SA simultaneously, and hence enhance the antagonism of SA. The physicochemical properties of CS nanoparticles were investigated using various analytical techniques such as transmission electron microscope (TEM), scanning electron microscope (SEM), X-ray diffraction (XRD) and FT-IR spectroscopy, and the drug release capability *in vitro* was also investigated.

2. Materials and methods

2.1. Materials

Chitosan (CS, Deacetylation degree 95%, molecular weight 80 kDa) was purchased from Golden-shell Biochemical Co. Ltd. (Zhejiang, China). Gentamicin was purchased from North China Pharmaceutical Co. Ltd. (Hebei, China). Salicylic acid was purchased from Hezhong Bio-Chemical Co. Ltd. (Wuhan, China). Tripolyphosphate was purchased from Wenzhou Dongsheng Chemical reagent Co. Ltd. (Zhengjiang, China). All other materials and reagents used in the study were analytical grade.

2.2. Preparation of compound CS nanoparticles

CS nanoparticles were prepared based on the ionic cross-linking of CS with TPP (Wu, Yang, Wang, Hu, & Fu, 2005). CS solution (0.2%, w/v) was prepared by dissolving CS in dilute acetic acid (1%, v/v) at room temperature with sonication. The CS solution with different pH ranging from 4.0 to 5.5 was flush mixed with certain volume of GM and SA solution (drug to polymer ratios of 1:1, 1:2, 1:3, 1:4, and 1:5). The CS nanoparticles formed spontaneously when the TPP solution was added to the mixture by dropwise. The selected mass ratios of CS to TPP were 3:1, 4:1, 5:1, 6:1, and 7:1. The nanoparticle suspensions were continuously stirred for 1 h and centrifuged at 16,000 rpm for 30 min. The resulting nanoparticle products were lyophilized and stored.

2.3. Characterization of GM/SA compound CS nanoparticles

The particle size, zeta potential and polydispersity index (PDI) of the nanoparticles obtained from Section 2.2 were measured by photon correlation spectroscopy using nano ZS90 Zetasizer (Malvern Instruments, UK). The samples were prepared with deionized water at appropriate concentrations. The surface morphology of the drug-loaded CS nanoparticles was observed by TEM and SEM. For TEM, the nanoparticles solution were dropped on copper grids, natively stained by phosphotungstic acid and dried at room temperature (Philips, Tecrai 10, Dutch). For SEM, the nanoparticle suspensions were spread on a glass plate and dried at room temperature. The dried nanoparticles were coated with gold metal under vacuum and then examined (Hitachi, S-3400N, Japan).

The chemical structure and complexes formation of CS, GM, SA and drug-loaded CS nanoparticles were analyzed by FT-IR (Nicolet, 5DX/550II, USA). The samples were prepared by grinding the dry specimens with KBr and pressing the mixed powder to form disks.

The XRD experiments were carried out using X-ray diffractometer (Shimadzu, XRD6000X, Japan). CS, GM, SA and drug-loaded CS nanoparticles were scanned from 5° to 40°.

2.4. Determination of drugs loading capacity of nanoparticles

GM consists of deoxystreptamine, purpurosamine and garamine. It has no specific absorption in the ultraviolet region. However, GM hydrolyzes quantitatively to aglycone and sugar under acidic condition or in phosphate buffer saline (PBS). The hydrolysate could be analyzed by UV spectrophotometry at 248 nm (Shimadzu, UV-2450, Japan). The content of SA was determined using UV spectrophotometry at 297 nm. Due to the weak ultraviolet absorption of SA at 248 nm, the differential spectrophotometry was used to calculate the amount of GM.

The encapsulation efficiency (EE) and loading capacity (LC) of the nanoparticles were determined according to the method described in the previous studies (Anal, Stevens, & Lopez, 2006). In brief, drug-loaded nanoparticles (20 mg) were extracted with 5 ml 0.1 mol/l HCl for 24 h at room temperature, and the nanoparticles suspensions were separated by centrifugation at 16,000 rpm for 30 min, the contents of GM and SA in the supernatants were measured by UV spectrophotometer at 248 nm and 297 nm, respectively. A blank sample was made from nanoparticles without loaded drugs (GM and SA) but treated similarly as the drug-loaded nanoparticles. All samples were measured in triplicate. The EE and LC were calculated by the following equations:

$$\mathrm{EE} = \frac{F}{T} \times 100\%$$

$$\mathrm{LC} = \frac{F}{W} \times 100\%$$

In the above equations, F is the free amount GM or SA in the supernatant, T is total amount of GM or SA, W is the weight of nanoparticles.

2.5. In vitro release studies

The *in vitro* release studies were carried out in PBS (pH 7.4) as followed: GM/SA loaded CS nanoparticles (30 mg) and 5 ml PBS were transferred into a dialysis tube (MWCO: 12,000). The dialysis tube was placed in 50 ml PBS at 37 °C and shaken at 100 stocks/min. At specific time intervals, medium was replaced with fresh PBS. Triplicate samples were analyzed at each time point. The concentrations of the released GM and SA into PBS were determined by UV spectrophotometer.

3. Results and discussion

3.1. Preparation of CS nanoparticles containing GM and SA

Preparation of the CS nanoparticles containing SA and GM with different mass ratios of CS to TPP from 3:1 to 7:1 was investigated. The concentration of CS was 0.2% (w/v). The feed mass ratio of SA (0.1%, w/v) to GM (0.2%, w/v) was selected as 1.5:1, and the pH of CS solution was 5.0. Table 1 shows the effect of CS/TPP mass ratios on the EE, LC, size and zeta potential values of CS nanoparticles. It was found that the EE and LC of the nanoparticles were decreased with increasing the CS/TPP mass ratios. Under the condition of maintaining constant amount of CS, the LC of the nanoparticles was higher in the case of the formulation containing higher amount of TPP and the size of nanoparticles also increased. The mean particle size of drug-loaded nanoparticles ranged from 150.8 ± 16.9 nm to 343.3 ± 12.4 nm, and the range of the PDI was from 0.237 to 0.414

Table 1
Effect of CS/TPP mass ratios on characteristics of the GM/SA-loaded CS nanoparticles (mean ± S. D., $n = 3$).

CS/TPP ratio	SA		GM		Size		Zeta potential (mV)
	EE (%)	LC (%)	EE (%)	LC (%)	nm	PDI	
3:1	81.30 ± 2.12	24.67 ± 2.06	87.20 ± 3.09	26.64 ± 3.92	343.3 ± 12.4	0.414	+34.26 ± 0.39
4:1	81.95 ± 2.51	22.27 ± 2.31	81.50 ± 3.51	23.88 ± 4.21	217.7 ± 9.5	0.275	+35.77 ± 0.07
5:1	72.45 ± 1.98	22.19 ± 2.39	78.30 ± 2.78	23.56 ± 2.61	180.0 ± 10.6	0.235	+37.12 ± 1.52
6:1	60.00 ± 3.21	20.61 ± 3.39	71.25 ± 1.59	20.42 ± 3.64	172.2 ± 15.2	0.308	+39.44 ± 1.09
7:1	59.45 ± 3.02	20.43 ± 3.54	61.70 ± 2.67	13.56 ± 3.50	150.8 ± 16.9	0.237	+42.43 ± 2.84

with a relatively narrow particle size distribution. The zeta potential of the nanoparticles was in the range of +34.26 ± 0.39 mV to +42.43 ± 2.84 mV and the positive zeta potential was due to the residual amine groups. The increases of mass ratio of CS to TPP led to an enhancement of particle surface charges.

The effect of different pH of CS solution (from 4.0 to 5.5) on the characteristics of compound nanoparticles was also investigated. The results are shown in Table 2. It demonstrates that the zeta potential of the nanoparticles decreased from +42.18 ± 1.44 mV to +35.39 ± 0.54 mV with increasing the pH of CS solution, which may be related to the decrease of the positive charges of CS. When the pH of CS solution values varied from 4.0 to 5.5, the average particle size of the nanoparticles increased from 148.2 ± 8.6 nm to 250.0 ± 15.5 nm, probably due to particle aggregation. The nanoparticles had a higher LC of SA at pH 4.0, the reason for this could be that the formulation pH was near the pK_a of SA (pK_a = 2.8) and the protonation of CS was enhanced at low pH (Boonsongrit, Mitrevej, & Mueller, 2006). In addition, a higher LC of GM was obtained at pH 5.0, which may be related to the sufficient anions of TPP and the positive charges of CS, and hence enhanced the degree of cross-link reaction.

CS nanoparticles with different drug-to-polymer ratios (1:1, 1:2, 1:3, 1:4 and 1:5) were also prepared in this study. Table 3 demonstrates that the EE of nanoparticles increased from 63.30 ± 3.98% to 79.80 ± 4.41% with decreasing the drug-to-polymer ratio. The LC of nanoparticles reached the highest value when the drug-to-polymer ratio was 1:4. The particle size was gradually decreased and a significant increase in the zeta potential was observed with reducing the drug-to-polymer ratio. This trend could be explained by the fact that the high zeta potential can prevent the particle from forming aggregation (Avadi et al., 2010).

Based on previous study (Song & Schacht, 1996), sufficient SA (the release amount ratio of SA to GM equal or higher than 1.0:1.2) was required to inhibit the ototoxicity of GM. CS nanoparticles loaded with GM and SA with the different feed drug ratios of SA to GM from 1.0:1.0 to 3.0:1.0 were also synthesized. As shown in Fig. 1, when the feed drug ratios of SA to GM increased from 1.0:1.0 to 3.0:1.0, the EE of SA decreased from 89.53% to 80.18% and the LC increased from 24.87% to 33.41%. The EE and LC of GM showed converse tendency.

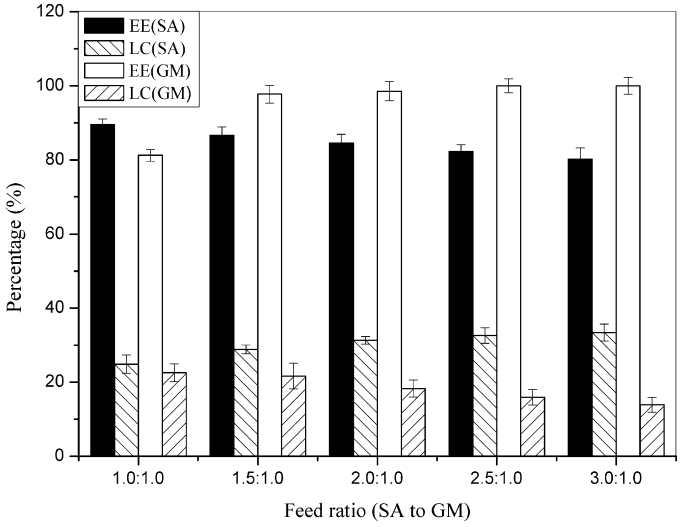

Fig. 1. The encapsulation efficiency and loading capacity of SA and GM with different feed ratios of SA to GM ($n = 3$).

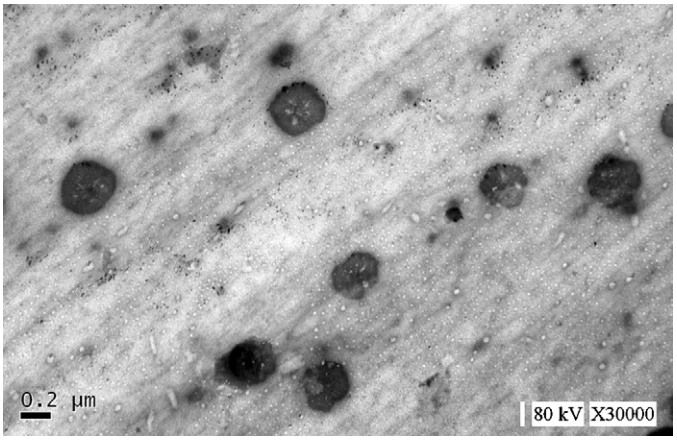

Fig. 2. TEM image of the SA/GM-loaded CS nanoparticles (CS/TPP ratio 4:1, pH 5.0, drug to polymer ratio 1:4, feed ratio of SA to GM 1.5:1.0).

3.2. Characterization of GM/SA-loaded CS nanoparticles

The morphological characteristics of the SA/GM-loaded CS nanoparticles were imaged using the TEM and SEM (Figs. 2 and 3). The pictures show that the GM/SA-loaded CS nanoparticles were spherical in shape, and the average size was about 200 nm.

Fig. 4 depicts the FT-IR spectra of CS, drugs loaded CS nanoparticles, GM and SA. The results demonstrate the basic structural features of CS (Fig. 4A) at 3426 cm^{-1} (–OH and –NH_2 stretching), 2922 cm^{-1} and 2872 cm^{-1} (–CH stretching), 1601 cm^{-1} (–NH_2 stretching), 1076 cm^{-1} (C–O–C stretching) and 601 cm^{-1} (pyranoside ring stretching vibration). For drugs loaded CS nanoparticles (Fig. 4B), the peak of 3423 cm^{-1} becomes wider, indicating that hydrogen bonding has been enhanced between the –OH group bending of GM at 3400 cm^{-1} (Fig. 4C) and CS (Wu et al., 2005). The –NH_2 bending vibration shifts from 1601 cm^{-1} to 1542 cm^{-1} and a new peak at 1637 cm^{-1} indicates that some interaction between NH_3^+ groups of CS and TPP have occurred within the nanoparticles (Xu & Du, 2003). The characteristic absorption peaks of SA (Fig. 4D) at 1700 cm^{-1} and 1650 cm^{-1} corresponds to acetoxy group and carboxylic group bending. The peak at 1300 cm^{-1} indicates the C–N group bending accounting for interaction between carboxylic –COOH group of SA and primary amide of chitosan, and the carboxylic group bending of SA about 1700 cm^{-1} may be overlapped. The results may indicate that SA and GM have been successfully loaded into the CS nanoparticles.

Table 2
Effect of pH values of CS solution on characteristics of the GM/SA-loaded CS nanoparticles (mean ± S. D., $n = 3$).

CS pH value	SA		GM		Particle size		Zeta potential (mV)
	EE (%)	LC (%)	EE (%)	LC (%)	nm	PDI	
4.0	76.45 ± 2.12	25.78 ± 1.05	66.00 ± 1.28	18.42 ± 1.79	148.2 ± 8.6	0.268	+42.18 ± 1.44
4.5	72.00 ± 3.25	22.34 ± 4.00	72.80 ± 1.56	17.35 ± 2.84	165.4 ± 11.9	0.234	+39.24 ± 1.12
5.0	72.45 ± 1.98	22.19 ± 2.39	78.30 ± 2.78	23.56 ± 2.61	180.0 ± 10.6	0.235	+37.12 ± 1.52
5.5	70.20 ± 3.05	20.28 ± 3.56	79.20 ± 3.65	21.97 ± 3.29	250.0 ± 15.5	0.240	+35.39 ± 0.54

Table 3
Effect of drug to polymer ratios on characteristics of the GM/SA-loaded CS nanoparticles (Mean ± S. D., $n = 3$).

Drug to polymer ratio	SA		GM		Particle size		Zeta potential (mV)
	EE (%)	LC (%)	EE (%)	LC (%)	nm	PDI	
1:1	63.30 ± 3.98	12.48 ± 2.87	65.00 ± 3.16	13.98 ± 3.21	345.0 ± 12.9	0.259	+32.45 ± 1.46
1:2	66.20 ± 2.65	18.46 ± 2.36	70.94 ± 5.02	18.68 ± 2.09	317.7 ± 15.2	0.249	+33.70 ± 3.07
1:3	70.00 ± 1.52	21.56 ± 2.54	76.65 ± 1.25	22.82 ± 2.54	257.1 ± 10.3	0.428	+35.70 ± 0.55
1:4	72.45 ± 1.98	22.19 ± 2.39	78.30 ± 2.78	23.56 ± 2.61	180.0 ± 10.6	0.235	+37.12 ± 1.52
1:5	72.60 ± 2.09	20.63 ± 1.12	79.80 ± 4.41	19.50 ± 2.49	156.5 ± 13.7	0.274	+42.07 ± 1.98

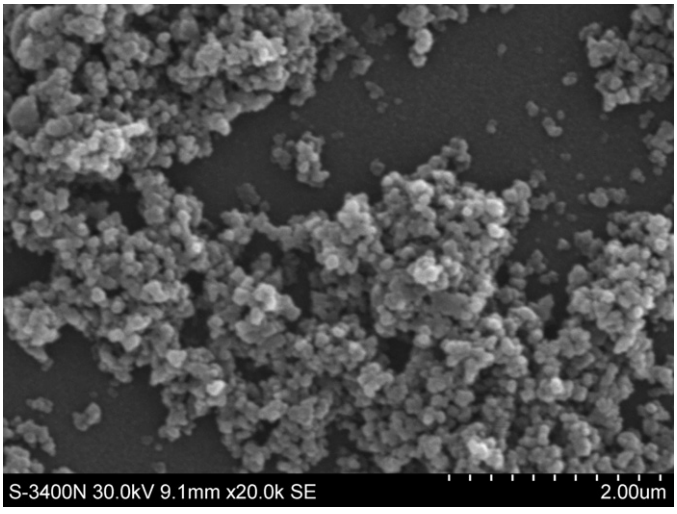

Fig. 3. SEM image of the SA/GM-loaded CS nanoparticles (CS/TPP ratio 4:1, pH 5.0, drug to polymer ratio 1:4, feed ratio of SA to GM 1.5:1.0).

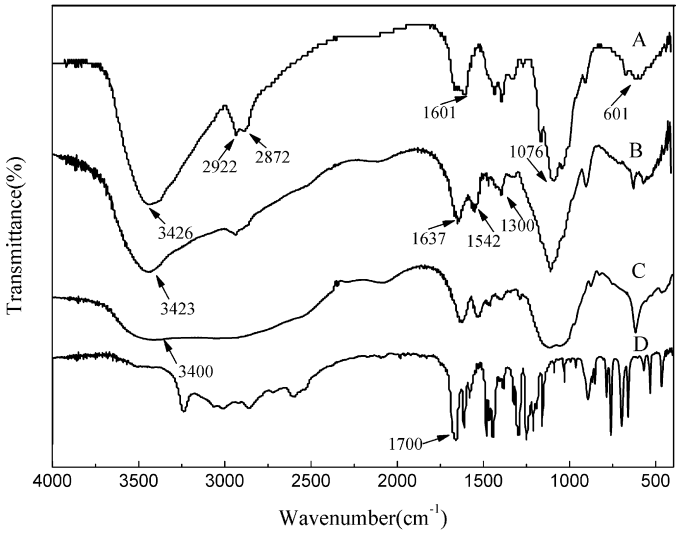

Fig. 4. FT-IR spectra of CS (A), SA/GM-loaded CS nanoparticles (B), gentamicin (C) and salicylic acid (D).

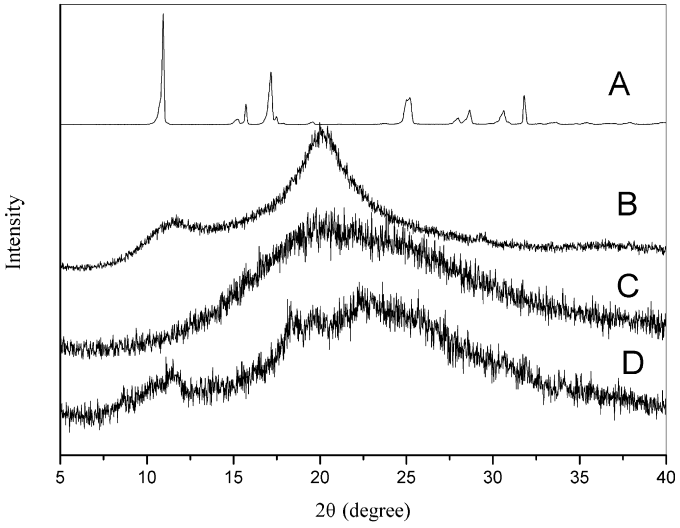

Fig. 5. XRD patterns of SA (A), CS (B), GM (C) and SA/GM-loaded CS nanoparticles (D).

The XRD patterns of CS, SA, GM and drugs loaded CS nanoparticles are illustrated in Fig. 5. There are four intense peaks in the diffractogram of SA at 2θ of 11°, 17°, 25° and 32.5° (Fig. 5A), which indicate the high degree of crystallinity. CS shows two peaks at 2θ of 11° and 20° (Fig. 5B), while GM has shown one peak at 2θ of 20° (Fig. 5C). After CS cross-linking with TPP (Fig. 5D), the basic diffraction peaks site were maintained and the peaks intensity decreased. Furthermore, the new peak at 2θ of 18° and 24° appeared, indicating that the crystal lattice was induced by ionic interaction (Yoksana, Jirawutthiwongchai, & Arpo, 2010). The specific sharp crystal peaks of SA and GM cannot be observed. The XRD peak depends on the crystal size, but the characteristic peaks of SA and GM may have overlapped with the noise of the coated polymer itself (Rokhade et al., 2006).

3.3. *In vitro release studies of GM/SA-loading CS nanoparticles*

The *in vitro* cumulative release profiles of GM and SA from the CS nanoparticles with different feed ratios of SA to GM (from 1.0:1.0 to 3.0:10) are shown in Figs. 6 and 7. The release profiles appeared to have three phases (Agnihotri & Aminabhavi, 2004). The first phase was a rapid release or burst release in the prior period with the

Table 4
Release kinetics of SA and GM released from CS nanoparticles with the different feed ratios of SA to GM.

Feed ratio (SA to GM)	SA					GM				
	First-order	Higuchi	Weibull	Korsmeyer–Peppas		First-order	Higuchi	Weibull	Korsmeyer–Peppas	
	r^2	r^2	r^2	r^2	n	r^2	r^2	r^2	r^2	n
1.0:1.0	0.802	0.806	0.958	0.963	0.352	0.781	0.830	0.972	0.911	0.429
1.5:1.0	0.759	0.806	0.945	0.991	0.481	0.843	0.851	0.980	0.930	0.467
2.0:1.0	0.704	0.786	0.917	0.988	0.508	0.871	0.834	0.981	0.920	0.551
2.5:1.0	0.704	0.804	0.870	0.991	0.446	0.879	0.824	0.989	0.842	0.430
3.0:1.0	0.788	0.890	0.942	0.959	0.384	0.888	0.811	0.990	0.918	0.386

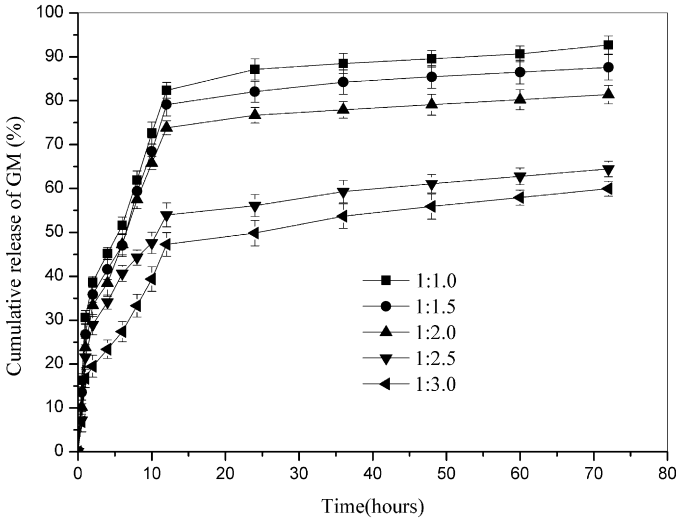

Fig. 6. *In vitro* release of GM from SA/GM-loaded CS nanoparticles with different feed ratio of SA to GM ($n = 3$).

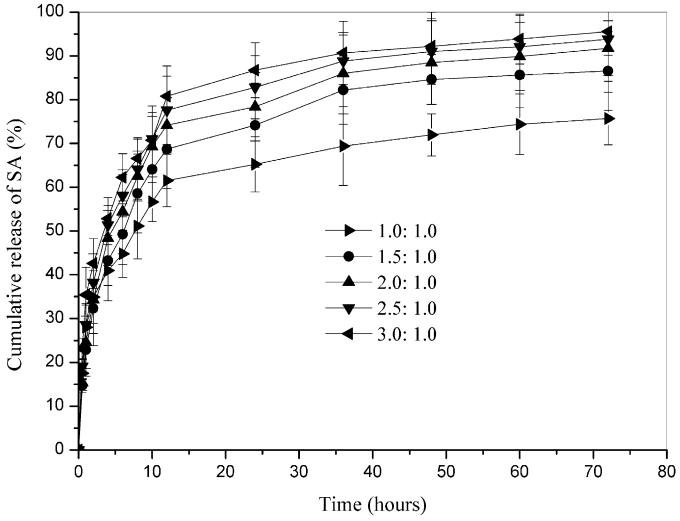

Fig. 7. *In vitro* release of SA from SA/GM-loaded CS nanoparticles with different feed ratio of SA to GM ($n = 3$).

sample of feed ratio 2.0:1.0, and about 45% SA and 38% GM were released in this phase (within the first 4 h). The rapid releasing process was mainly due to the nanoparticles surface drugs could easily diffuse in the initial time. The second phase was a relatively slow release ranging from 4 to 12 h, which could be caused by the drugs diffused from the matrix. About 87% SA and 81% GM were released in this phase. The third phase was a slower releasing process due to the polymer degradation. The dissolved drugs were diffused into the release medium. The cumulative percentage release of SA and GM from the compound nanoparticles was about 95% and 92% for 72 h, respectively.

The release rate was higher in the case of formulations containing higher amount of drugs, and similarly, drug release was lower for formulations having a lower amount of drugs (Rokhade, Patil, & Aminabhavi, 2007). Thus, the release rate of SA increased with increasing the feed ratio of SA to GM from 1.0:1.0 to 3.0:1.0, and the release rate of GM decreased. The release amount ratios of SA to GM depending upon the different feed ratios were also investigated in the *in vitro* release studies. The release amount ratios of SA to GM were nearly 1.0:1.0 in 72 h, which was higher than 1.0:1.2. This may contribute to maintaining a high blood concentration of SA *in vivo* and reducing the injection times.

Data obtained from the *in vitro* release studies were fitted to various kinetic equations such as first-order, Higuchi model and Weibull model. The results are shown in Table 4. The optimum model was selected based on the correlation coefficient value (r^2) of various model, and the results indicated that the drugs release from nanoparticles fitted Weibull model best from the above three models.

The Korsmeyer–Peppas equation was also used to determine the mechanism of drug release. The initial portion (i.e., $M_t/M_\infty \leq 60\%$) of cumulative drug release (%) vs. time can be expressed by followed equation (Kumbar, Soppimath, & Aminabhavi, 2003):

$$\frac{M_t}{M_\infty} = Kt^n$$

where M_t/M_∞ is the fraction of drug released at time t, k is the kinetic constant and n is the diffusion exponent; the n value was calculated and presented in Table 4. For the formulation with the feed ratio 2.0:1.0, the n value of the SA was 0.508 and the trend was corresponding to Fickian diffusion. The drug release for others formulations deviated slightly from Fickian trend following anomalous or non-Fickian trends (Mundargi et al., 2008; Wilson et al., 2010).

4. Conclusion

The GM and SA loaded CS nanoparticles were successfully prepared by cross-linking with TPP. The nanoparticles were stable and spherical in shape with a narrow size distribution. Different percentage entrapment efficiency and loading efficiency of GM and SA were obtained by varying the mass ratio of CS to TPP, the drug to polymer ratio, the pH of CS solution and the feed ratio of SA to GM. The *in vitro* release studies indicated that the feed ratio of SA to GM influenced the release rate of GM and SA from the CS nanoparticles and the release mechanism followed a non-Fickian type behavior. The release amounts of SA and GM from the CS nanoparticles suggested that SA and GM loaded CS nanoparticles have promising potential effect on antagonism ototoxicity of GM.

Acknowledgements

Thus research was supported by Chongqing University Postgraduates' Science and Innovation Fund (201005A1A0010333) and 211 Project Innovation Personnel Training Plan Items of Chongqing University (S-09103). We would like to thank Lu Ju and Li Fei (Laboratory of Electron Microscopy of Third Military Medical University) for they help in the nanoparticles characterization by SEM and TEM.

References

Agnihotri, S. A., & Aminabhavi, T. M. (2004). Controlled release of clozapine through chitosan microparticles prepared by a novel method. *Journal of Controlled Release*, *96*, 245–259.

Agnihotri, S. A., Mallikarjuna, N. N., & Aminabhavi, T. M. (2004). Recent advances on chitosan-based micro- and nanoparticles in drug delivery. *Journal of Controlled Release*, *100*, 5–28.

Anal, A. K., Stevens, W. F., & Lopez, C. R. (2006). Ionotropic cross-linked chitosan microspheres for controlled release of ampicillin. *International Journal of Pharmaceutics*, *312*, 166–173.

Atyabi, F., Moghaddam, F. A., Dinarvand, R., ZohuriaanMehr, M. J., & Ponchel, G. (2008). Thiolated chitosan coated poly hydroxyethyl methacrylate nanoparticles: synthesis and characterization. *Carbohydrate Polymers*, *74*, 59–67.

Avadi, M. R., Sadeghi, A. M. M., Mohammadpour, M., Abedin, S., Atyabi, F., Dinarvand, R., et al. (2010). Preparation and characterization of insulin nanoparticles using chitosan and Arabic gum with ionic gelation method. *Nanomedicine: Nanotechnology, Biology and Medicine*, *6*, 58–63.

Boonsongrit, Y., Mitrevej, A., & Mueller, B. W. (2006). Chitosan drug binding by ionic interaction. *European Journal of Pharmaceutics and Biopharmaceutics*, *62*, 267–274.

Chen, Y., Huang, W. G., Zha, D. J., Qiu, J. H., Wang, J. L., Sha, S. H., et al. (2007). Aspirin attenuates gentamicin ototoxicity: from the laboratory to the clinic. *Hearing Research*, *226*, 178–182.

Cooney, M. J., Petermann, J., Lau, C., & Minteer, S. D. (2009). Characterization and evaluation of hydrophobically modified chitosan scaffolds: towards design of enzyme immobilized flow-through electrodes. *Carbohydrate Polymers*, *75*, 428–435.

Fan, M., Hu, Q. L., & Shen, K. (2009). Preparation and structure of chitosan soluble in wide Ph range. *Carbohydrate Polymers*, *78*, 66–71.

Fu, X. F., Huang, L., Zhai, M. L., Li, W., & Liu, H. W. (2007). Analysis of natural carbohydrate biopolymer-high molecular chitosan and carboxymethyl chitosan by capillary zone electrophoresis. *Carbohydrate Polymers*, *68*, 511–516.

Gan, Q., Wang, T., Cochrane, C., & McCarron, P. (2005). Modulation of surface charge, particle size and morphological properties of chitosan–TPP nanoparticles intended for gene delivery. *Colloids and Surfaces B: Biointerfaces*, *44*, 65–73.

Govender, T., Riley, T., Ehtezazi, T., Garnett, M. C., Stolnik, S., Illum, L., et al. (2000). Defining the drug incorporation properties of PLA–PEG nanoparticles. *International Journal of Pharmaceutics*, *199*, 95–110.

Hirose, K., Hockenbery, D. K., & Rubel, E. W. (1997). Reactive oxygen species in chick hair cells after gentamicin exposure in vitro. *Hearing Research*, *104*, 1–14.

Kumari, A., Yadav, S. K., & Yadav, S. C. (2010). Biodegradable polymeric nanoparticles based drug delivery systems. *Colloids and Surfaces B: Biointerfaces*, *75*, 1–18.

Kumbar, S. G., Soppimath, K. S., & Aminabhavi, T. M. (2003). Synthesis and characterization of polyacrylamide-grafted chitosan hydrogel microspheres for the controlled release of indomethacin. *Journal of Applied Polymer Science*, *87*, 1525–1536.

Lautermann, J., McLaren, J., & Schacht, J. (1995). Glutathione protection against gentamicin ototoxicity depends on nutritional status. *Hearing Research*, *86*, 15–24.

Lin, H. Y., & Chou, C. C. (2004). Antioxidative activities of water-soluble disaccharide chitosan derivatives. *Food Research International*, *37*, 883–889.

Maekawa, H., Matsunobu, T., Tsuda, H., Onozato, K., Masuda, Y., Tanabe, T., et al. (2009). Therapeutic effect of edaravone on inner ear barotrauma in the guinea pig. *Neurochemistry International*, *54*, 513–518.

McFadden, S. L., Ding, D. L., Salvemini, D., & Salvi, R. J. (2003). M40403, a superoxide dismutase mimetic, protects cochlear hair cells from gentamicin, but not cisplatin toxicity. *Toxicology and Applied Pharmacology*, *186*, 46–54.

Mundargi, R. C., Shelke, N. B., Rokhade, A. P., Sangamesh, A., Patil, S. A., & Aminabhavi, T. M. (2008). Formulation and in-vitro evaluation of novel starch-based tableted microspheres for controlled release of ampicillin. *Carbohydrate Polymers*, *71*, 42–53.

No, H. K., Kim, S. H., Lee, S. H., Park, N. Y., & Prinyawiwatkul, W. (2006). Stability and antibacterial activity of chitosan solutions affected by storage temperature and time. *Carbohydrate Polymers*, *65*, 174–178.

Peesan, M., Supaphol, P., & Rujiravanit, R. (2005). Preparation and characterization of hexanoyl chitosan/polylactide blend films. *Carbohydrate Polymers*, *60*, 343–350.

Polat, A., Parlakpinar, H., Tasdemir, S., Colak, C., Vardi, N., Ucar, M., et al. (2006). Protective role of aminoguanidine on gentamicin-induced acute renal failure in rats. *Acta Histochemica*, *108*, 365–371.

Rokhade, A. P., Agnihotri, S. A., Patil, S. A., Mallikarjuna, N. N., Kulkarni, P. V., & Aminabhavi, T. M. (2006). Semi-interpenetrating polymer network microspheres of gelatin and sodium carboxymethyl cellulose for controlled release of ketorolac tromethamine. *Carbohydrate Polymers*, *65*, 243–252.

Rokhade, A. P., Shelke, N. B., Patil, S. A., & Aminabhavi, T. M. (2007). Novel interpenetrating polymer network microspheres of chitosan and methylcellulose for controlled release of theophylline. *Carbohydrate Polymers*, *69*, 678–687.

Ryals, B., Westbrook, E., & Schacht, J. (1997). Morphological evidence of ototoxicity of the iron chelator deferoxamine. *Hearing Research*, *112*, 44–48.

Severinsen, S. A., Kirkegaard, M., & Nyengaard, J. R. (2006). 2,3-Dihydroxybenzoic acid attenuates kanamycin-induced volume reduction in mouse utricular type I hair cells. *Hearing Research*, *212*, 9–108.

Sha, S. H., & Schacht, J. (2000). Antioxidants attenuate gentamicin-induced free radical formation in vitro and ototoxicity in vivo: D-methionine is a potential protectant. *Hearing Research*, *142*, 34–40.

Song, B. B., & Schacht, J. (1996). Variable efficacy of radical scavengers and iron chelators to attenuate gentamicin ototoxicity in guinea pig in vivo. *Hearing Research*, *94*, 87–93.

Song, B. B., Sha, S. H., & Schacht, J. (1998). Iron chelators protect from aminoglycoside induced cochleo and vestibulo toxicity. *Free Radical Biology & Medicine*, *25*, 189–195.

Talaska, A. E., Schacht, J., & Nathan, F. G. (2006). Molecular and genetic aspects of aminoglycoside-induced hearing loss. *Drug Discovery Today: Disease Mechanisms Hearing disorders*, *3*, 119–124.

Wan, A. J., Sun, Y., Gao, L., & Li, H. L. (2009). Preparation of aspirin and probucol in combination loaded chitosan nanoparticles and in vitro release study. *Carbohydrate Polymers*, *75*, 566–574.

Wang, X. M., Chi, N., & Tang, X. (2008). Preparation of estradiol chitosan nanoparticles for improving nasal absorption and brain targeting. *European Journal of Pharmaceutics and Biopharmaceutics*, *70*, 735–740.

Wilson, B., Samanta, M. K., Santhi, K., Kumar, K. P. S., Ramasamy, M., & Suresh, B. (2010). Chitosan nanoparticlesasa new delivery system for the anti-Alzheimer drug tacrine. *Nanomedicine: Nanotechnology, Biology and Medicine*, *6*, 144–152.

Wu, W., Yang, W., Wang, C. C., Hu, J. H., & Fu, S. K. (2005). Chitosan nanoparticles as a novel delivery system for ammonium glycyrrhizinate. *International Journal of Pharmaceutics*, *295*, 235–245.

Xu, Y. M., & Du, Y. M. (2003). Effect of molecular structure of chitosan on protein delivery properties of chitosan nanoparticles. *International Journal of Pharmaceutics*, *250*, 215–226.

Yoksana, R., Jirawutthiwongchai, J., & Arpo, K. (2010). Encapsulation of ascorbyl palmitate in chitosan nanoparticles by oil-in-water emulsion and ionic gelation processes. *Colloids and Surfaces B: Biointerfaces*, *76*, 292–297.